



Contents lists available at ScienceDirect

Bioorganic & Medicinal Chemistry

journal homepage: www.elsevier.com/locate/bmc

A diazirine-based photoaffinity etoposide probe for labeling topoisomerase II

Gaik-Lean Chee^{a,*}, Jack C. Yalowich^b, Andrew Bodner^b, Xing Wu^a, Brian B. Hasinoff^a^a Faculty of Pharmacy, University of Manitoba, Winnipeg, Manitoba, Canada R3E 0T5^b Department of Pharmacology and Chemical Biology, University of Pittsburgh School of Medicine, Pittsburgh, PA 15261, United States

ARTICLE INFO

Article history:

Received 27 August 2009

Revised 13 November 2009

Accepted 21 November 2009

Available online 27 November 2009

Keywords:

Photoaffinity labeling

Etoposide

Topoisomerase II

Diazirine

ABSTRACT

Etoposide is a widely used anticancer drug that targets topoisomerase II, an essential nuclear enzyme. However, despite the fact that it has been in use and studied for more than 30 years the specific site on the enzyme to which it binds is unknown. In order to identify the etoposide binding site(s) on topoisomerase II, a diazirine-based photoaffinity etoposide analog probe has been synthesized and its photo-reactivity and biological activities have been characterized. Upon UV irradiation, the diazirine probe rapidly produced a highly reactive carbene species that formed covalent adducts containing stable carbon-based bonds indicating that it should also be able to form stable covalent adducts with amino acid residues on topoisomerase II. The human leukemia K562 cell growth and topoisomerase II inhibitory properties of the diazirine probe suggest that it targets topoisomerase II in a manner similar to etoposide. The diazirine probe was also shown to act as a topoisomerase II poison through its ability to cause topoisomerase II α -mediated double-strand cleavage of DNA. Additionally, the diazirine probe significantly increased protein–DNA covalent complex formation upon photoirradiation of diazirine probe-treated K562 cells, as compared to etoposide-treated cells. This result suggests that the photoactivated probe forms a covalent adduct with topoisomerase II α . In conclusion, the present characterization of the chemical, biochemical, and biological properties of the newly synthesized diazirine-based photoaffinity etoposide analog indicates that use of a proteomics mass spectrometry approach will be a tractable strategy for future identification of the etoposide binding site(s) on topoisomerase II through covalent labeling of amino acid residues.

© 2009 Elsevier Ltd. All rights reserved.

1. Introduction

Etoposide (Fig. 1A) has been one of the most widely used anticancer drugs in the world in the past three decades.^{1–3} The cellular target of etoposide has been identified to be DNA topoisomerase II, an essential nuclear enzyme required for regulating the topology of DNA.^{4–6} The drug acts on topoisomerase II by stabilizing the intermediate topoisomerase II-cleaved DNA covalent complexes (also referred to as cleavage complexes), converting the enzyme into a highly potent cellular toxin which triggers irreversible apoptotic processes.^{7–9} Even though over two thousand structurally related analogs have been prepared and numerous studies have been conducted to elucidate the drug–enzyme molecular interaction and structure–activity requirements for this drug class, the details of the binding sites are still unknown. This information could be particularly useful in the design of new etoposide analogs using a structure-based approach as various X-ray crystal structures of topoisomerase II are now available.^{10–15} Structure-based design is an attractive approach for the epipodophyllotoxin drug class considering that only two closely related clinically useful analogs,

teniposide and etoposide phosphate, have been introduced after nearly four decades of drug optimization using a ligand-based approach. Teniposide, a more lipophilic analog of etoposide, was developed as a means to facilitate cellular drug uptake,^{16,17} whereas etoposide phosphate is a hydrolysable prodrug of etoposide that was designed to improve the aqueous solubility of the drug.^{3,18}

Several techniques have been employed to locate drug binding sites on proteins. Among them, photoaffinity labeling using a photolabile probe is particularly useful because of the ability of the probe to photochemically form a covalent adduct with the target protein. The labeled amino acid residue in the binding site may then be identified using a proteomics mass spectrometry approach. Etoposide has been shown to bind to topoisomerase II in the absence of DNA with an apparent dissociation constant in the low micromolar range.^{19,20} This binding ability should allow the use of photoaffinity labeling as a method to identify the etoposide binding sites. We previously developed a photoactivatable azido analogue of etoposide (**1** in Fig. 1A) for probing the drug binding sites on topoisomerase II.²¹ However, our attempts to identify the photochemically labeled amino acid residues of topoisomerase II α using matrix-assisted laser desorption/ionization mass spectrometry (MALDI-MS) were unsuccessful, presumably due to the

* Corresponding author. Tel.: +1 204 272 1589; fax: +1 204 474 7617.
E-mail address: lean_chee@umanitoba.ca (G.-L. Chee).

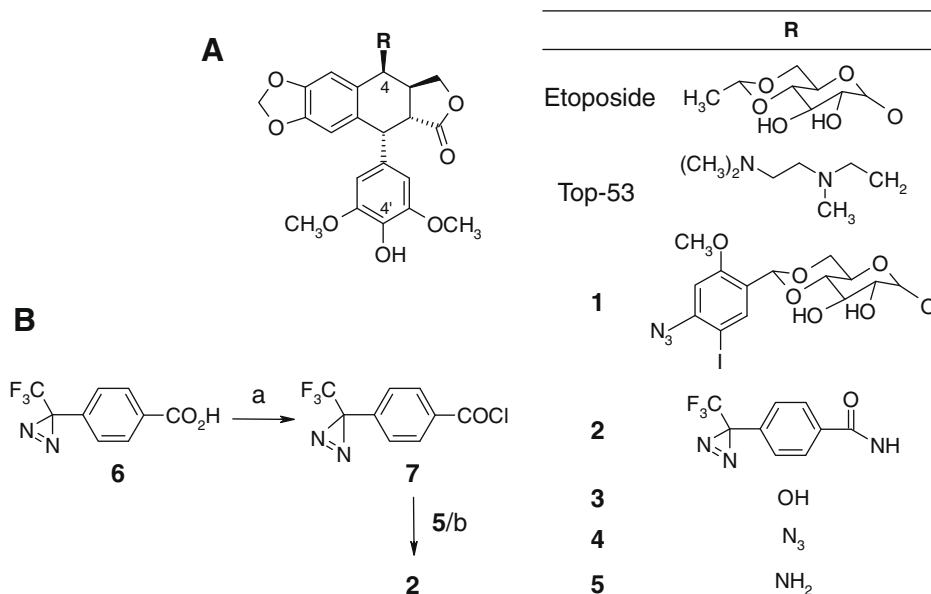


Figure 1. (A) Selected structures of 4'-demethyl-4 β -podophyllotoxin derivatives. (B) The synthetic scheme of diazidine **2**; (a) SOCl₂, room temperature, and (b) pyridine/ethyl acetate, room temperature.

loss of the etoposide probe under MALDI conditions (unpublished results). It is likely that the azido probe formed a drug–enzyme covalent adduct with a labile nitrogen–heteroatom linkage that was cleaved at high temperature.^{22,23}

As part of our ongoing effort to identify the etoposide binding sites on topoisomerase II, we have synthesized a new photoaffinity etoposide probe containing a 3-trifluoromethyl-3-aryldiazirine photophore (**2** in Fig. 1A). The diazirine photophores have gained popularity over the other photoreactive groups due to their highly desirable properties as photoaffinity probes.²⁴ In particular, the diazirines undergo rapid photoactivation into highly reactive carbene species that can even form carbon–carbon covalent bonds with aliphatic hydrocarbons. The fact that the photoactivated diazirines produce photoadducts with stable carbon–based covalent bonds should overcome the challenges we previously encountered with azido **1** in identifying the labeled amino acid residues. In this report, we describe the synthesis, photochemical reactivity, and biological activities of diazidine **2**, and also demonstrate the potential usefulness of this photoaffinity probe for identifying the etoposide binding sites on topoisomerase II.

2. Results

2.1. Chemical synthesis and photochemical kinetics in organic solvents

Photoaffinity etoposide probe, diazidine **2**, was prepared from amine **5**²⁵ and commercially available benzoic acid **6** in an overall yield of 41% (Fig. 1B). The photochemical reactions of diazidine **2** were performed to examine the reactivity of **2** upon photoactivation and to define the reaction conditions required for high-yield photolabeling of topoisomerase II. The photochemical kinetics of diazidine **2** in methanol at 365 nm for fixed periods of time was followed spectrophotometrically (Fig. 2). The diazidine group of **2** showed a characteristic absorbance peak at about 348 nm, consistent with the spectral properties of other reported 3-trifluoromethyl-3-aryldiazirines.^{26–29} Upon UV irradiation, the absorbance at 348 nm decreased with a half-life of about 40 s following approximately first-order kinetics (Fig. 2B) as has been reported

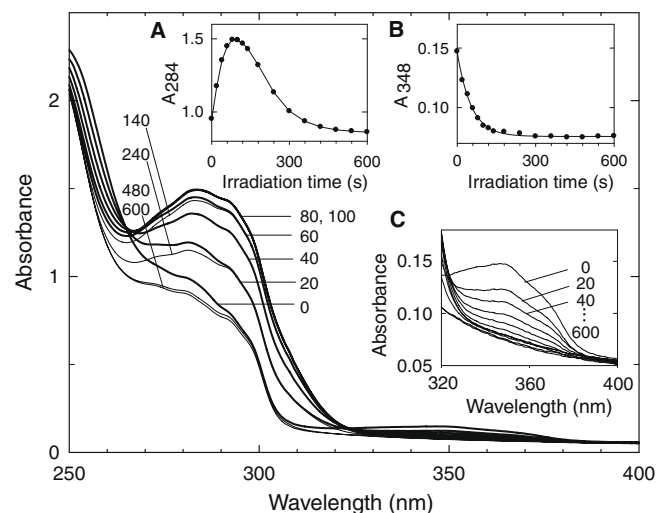


Figure 2. UV–vis spectral changes that occurred upon the irradiation of diazidine **2** for increasing periods of time (in s) as indicated. The irradiation was carried out in methanol at a concentration of 80 μ M in a 1-cm silica spectrometer cell at 365 nm (4.5 mW/cm² output). The thick and thin lines show the absorbance increase and decrease in the region of 270–320 nm, respectively. Insets (A) and (B) show the absorbance changes at 284 and 348 nm, respectively, as a function of irradiation time. Inset (C) is the expanded plot for the diazidine characteristic region of 320–400 nm.

for other diazirines.³⁰ The decrease in absorbance reflects the conversion of diazidine **2** into other species. While the absorbance at 348 nm decreased, the absorbance at 284 nm increased rapidly during the first 100 s (Fig. 2A). This has been attributed to the initial production of a diazo isomer by photochemical rearrangement of the diazidine moiety, as previously observed for other diazidine compounds.^{29,31} Upon further irradiation, the diazo isomer underwent further photolysis and the absorbance changes were nearly complete by 600 s. Diazidine **2** also underwent complete photolysis at 365 nm in about 600 s in ethyl acetate and acetonitrile (data not shown). The reactions in these two solvents produced similar spectral changes and similar first order kinetics as the photolysis performed in methanol (data not shown).

2.2. LC–MS/MS analysis of photolysis products produced in organic solvents

The photolysis of diazirine **2** in organic solvents was further examined by analyzing the photoproducts produced using LC–MS/MS. Photolysis of **2** in methanol at 365 nm for 120 s afforded four peaks in the total ion chromatogram shown in Figure 3B. Electrospray ionization (ESI) MS/MS analysis (Fig. 4B–E) of these four peaks was consistent with compounds **2**, **8**, **9** and **10/11** being present (structures in Fig. 4A). High abundances of $[M+H]^+$ and $[M+Na]^+$ were observed in the LC–MS mode for all these compounds, suggesting that they were highly stable under the ESI–MS conditions. This also implies that the covalent adduct of diazirine **2** and topoisomerase II peptide will be stable under our proposed MALDI experiments. Upon applying moderate collision energy in the MS/MS mode, the molecular ions of these compounds underwent minor fragmentations to afford daughter ions that further substantiated the proposed structures (Fig. 4B–E).

The chromatographic peak with the longest retention time in Figure 3B is assigned to diazirine **2** as it corresponds to the retention time observed for the unphotolyzed diazirine (Fig. 3A). The appearance of two major daughter ions, m/z 584 and 383, in the mass spectrum (Fig. 4B) corresponding to this peak in Figure 3B, likely resulted from the loss of a molecular nitrogen and the whole benzoyl amide fragment from **2**, respectively (Fig. 5A). The structures of these daughter ions are proposed to be **14a** and **16** as shown in Figure 5F. Fragment **14a** is likely the carbene intermediate generated thermally under ESI conditions. The structure of **16** has been previously proposed for the MS fragmentations of 4'-demethylpodophyllotoxin derivatives.³² The observation of these two daughter ions supports the proposal that the compound is diazirine **2**.

The compound that eluted immediately before diazirine **2** (Fig. 3B) is proposed to be the photorearrangement isomer, diazo **8**. The observation that **8** had a slightly shorter retention time than **2** is consistent with **8** being a more polar compound than **2**. In addition, the MS/MS spectrum corresponding to this peak (Fig. 4C) shows a similar fragmentation pattern to that of diazirine **2** (Fig. 4B), which is consistent with diazo **8** having the same molecular weight as and significant structural resemblance to diazirine **2**. These results also demonstrated the ability of **8** to form a carbene (**14a**) when thermally activated, as previously reported for other diazo compounds.³³

The chromatographic peak with the 4.4 min retention time in Figure 3B is assigned to photoadduct **9**. The primary fragmentation pathway of **9** also resembled that of **2** and **8**, affording two major daughter ions with m/z 584 and 383 (Fig. 4D). However, m/z 584

was the result of the loss of 32 amu from $[9+H]^+$, which corresponds to the loss of a methanol molecule (Fig. 5B).

The identity of the most polar component in the chromatogram shown in Figure 3B is suggested to be either **10** or **11**. The actual structure for this component could not be conclusively determined by analyzing the MS/MS spectrum shown in Figure 4E because both **10** and **11** have molecular ions with m/z 618. In addition, both structures could result in two primary fragmentation pathways that give m/z 616 and 586 as shown in Figure 4E. The loss of 2 and 32 amu from m/z 618 is proposed to be attributable to H_2 and O_2 , giving rise to dioxirane **14b** and alkane **14d**, respectively (Fig. 5C). Even though the structure of this photoadduct was not conclusively determined, it is likely that either **10** or **11** is a covalent adduct resulted from the reaction between the photogenerated carbene intermediate and dissolved molecular oxygen or water, respectively.

In summary, the LC–MS/MS study of the photolysis of **2** in methanol at 365 nm reveals that the photolysis was only partially complete by 120 s, affording the unreacted diazirine **2**, photorearrangement isomer **8**, and photoadducts **9** and **10/11**. However, continuous irradiation of **2** for 600 s led to complete photolysis that produced only photoadducts **9** and **10/11** as shown in Figure 3C. Based on our observations on the photolysis of **2** in methanol and the general photolytic pathway suggested for the 3-trifluoromethyl-3-aryldiazirine group,^{24,31} the photolytic pathway for **2** is summarized in Figure 3E. Since the diazo isomers are known to be more efficiently activated at 302 nm to yield carbene intermediates,³⁴ we also examined the photochemical reactions at both 365 and 302 nm to improve the photolysis efficiency. Photoirradiation at 365 nm for 90 s followed by 302 nm for 30 s (Fig. 3D) was found to be nearly as efficient as continuous irradiation at 365 nm for 600 s (Fig. 3C) for producing photoadducts **9** and **10/11**.

The photolysis products of diazirine **2** in ethyl acetate and acetonitrile were also examined to further investigate the reactivity of the carbene intermediate generated from **2** photochemically. According to the LC–MS/MS analysis (data not shown), the photolysis of diazirine **2** in ethyl acetate and acetonitrile at 365 nm for 600 s afforded two major photoadducts that are proposed to be **12** and **13**, respectively. Several other minor photoproducts were also observed but were uncharacterized due to poor chromatographic separation. Diazirine **2** and diazo **8** were not detected in the reaction mixture, indicating the completion of the reactions. High abundances of $[M+H]^+$ and $[M+Na]^+$ in the LC–MS mode were also observed for **12** and **13** (Fig. 4A). The MS/MS spectrum of photoadduct **12** shows three major daughter ions, m/z 670, 640 and 638, in addition to the molecular ion observed (Fig. 4F). The loss of 2 amu from **12** suggests that m/z 670 is an H_2 elimination prod-

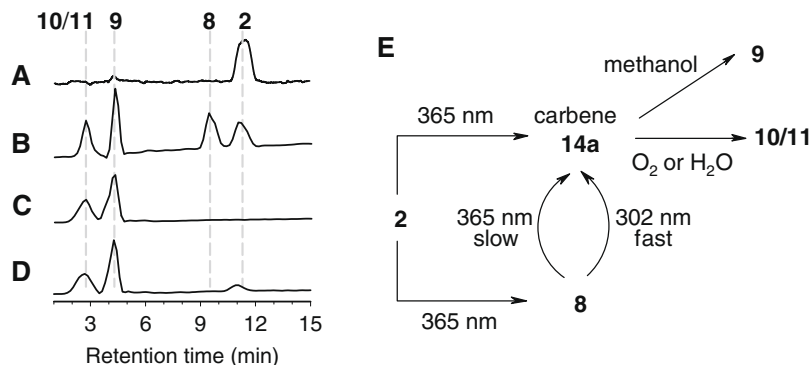


Figure 3. LC–MS/MS total ion chromatograms of the photolyzed solution and proposed photolytic pathway of diazirine **2** in methanol. (A) Diazirine **2** before photolysis. (B) 365 nm for 120 s. (C) 365 nm for 600 s. (D) 365 nm for 90 s followed by 302 nm for 30 s. (E) Photolytic pathway of diazirine **2**, where **2** is proposed to give rise to a carbene intermediate (**14a** in Fig. 5F) and the competing side product diazo **8** that undergoes further photolysis to **14a**. Subsequent reactions of **14a** with methanol and molecular oxygen or water produce **9** and **10/11**, respectively, as final photolysis products. The chemical structures of **8–11**, and **14a** are provided in Figures 4 and 5, respectively.

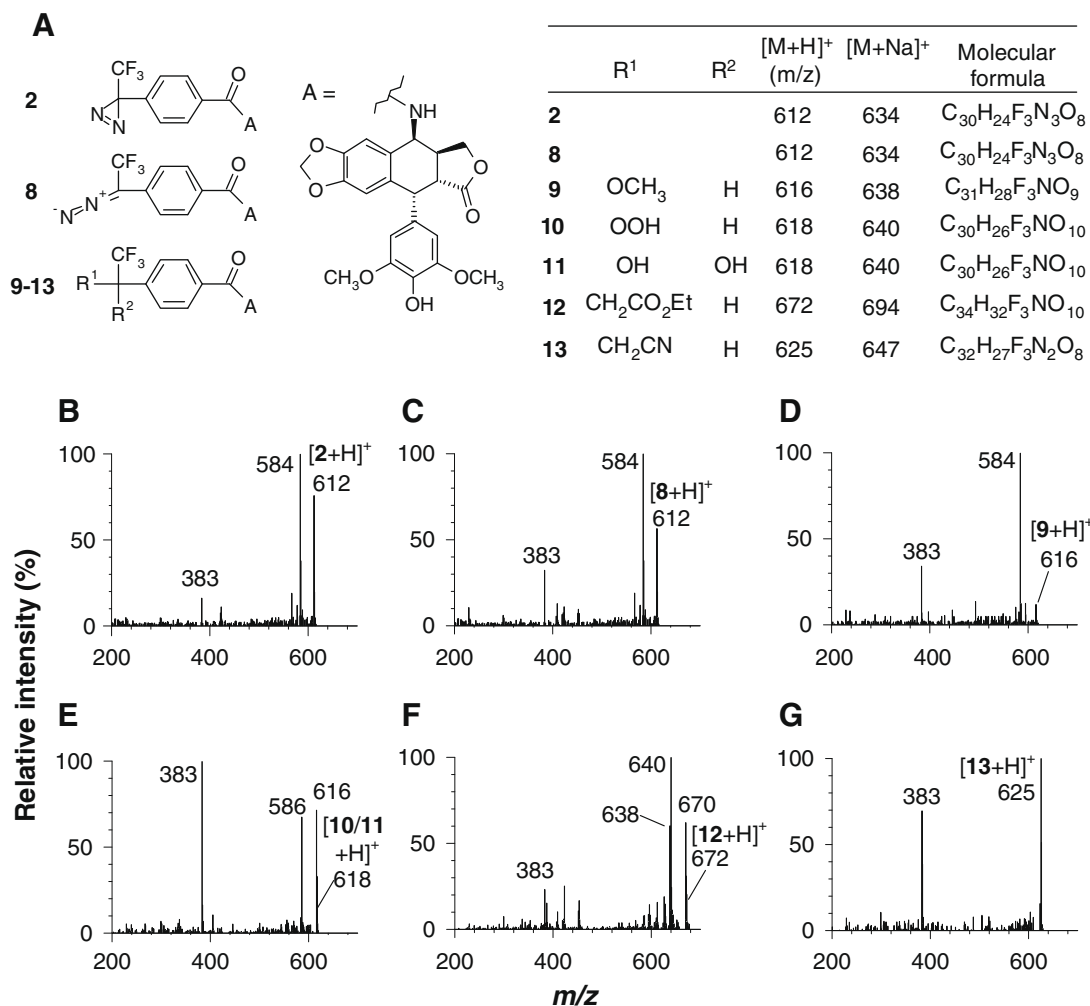


Figure 4. Compounds present in the photolyzed solutions of **2** in different organic solvents. (A) Proposed structures, masses of molecular ions observed in the LC–MS mode, and molecular formula for these compounds. (B)–(G) are MS/MS spectra that correspond to the chromatographic peaks of diazirine **2**, diazo **8**, **9**, **10/11**, **12**, and **13**, respectively.

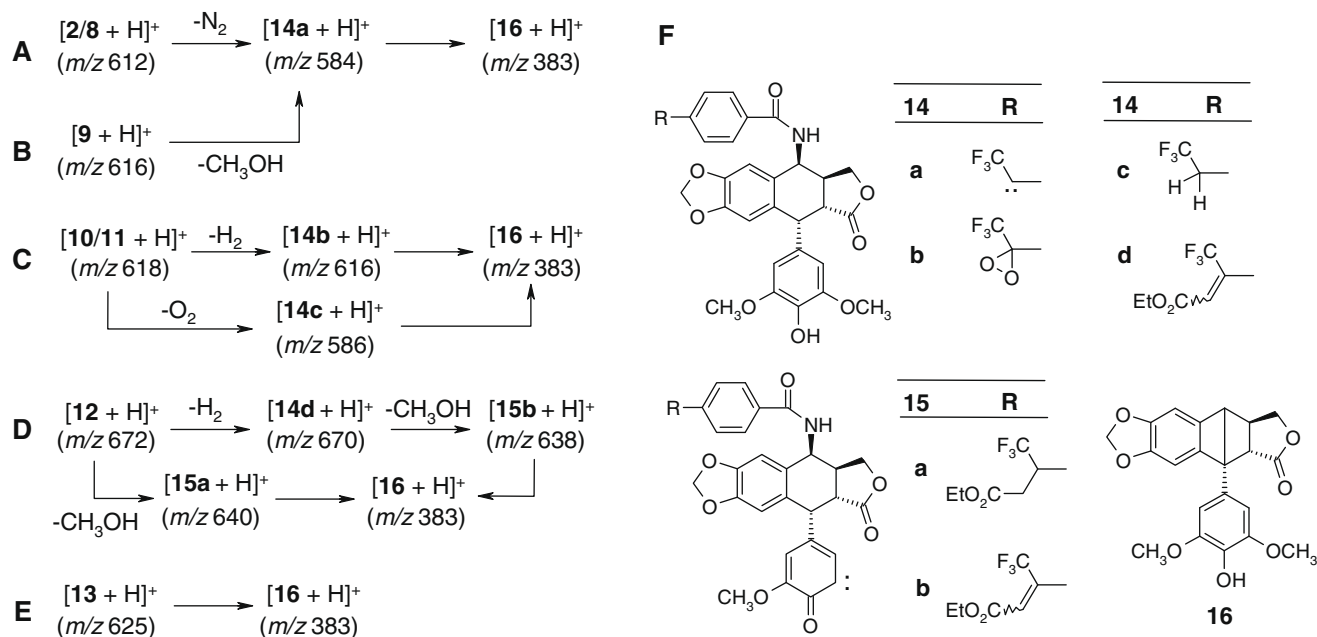


Figure 5. Proposed MS/MS fragmentation pathways for **2/8**, **9**, **10/11**, **12**, and **13**, as shown in (A)–(E), respectively. (F) Proposed structures of the major daughter ions observed in the MS/MS spectra of diazirine **2** and its photoproducts.

uct **14d** (Fig. 5D and F). Both **12** and **14d** could undergo fragmentations through the loss of a methanol molecule to afford fragment ions m/z 640 and 638, which are proposed to be **15a** and **15b**, respectively. The daughter ions observed clearly support the structure we proposed for **12**. Unlike **12**, the proposed acetonitrile photolysis product **13** afforded a simple fragmentation pattern (Fig. 4G) that showed only the molecular ion m/z 625 and a dominant daughter ion m/z 383 which has already been proposed to be $[16+H]^+$ (Fig. 5E and F). Our results demonstrated the strong reactivity of diazirine **2** upon UV irradiation, generating a carbene intermediate that subsequently formed highly stable carbon–carbon covalent bonds with ethyl acetate and acetonitrile.

2.3. K562 cell growth inhibition

Etoposide has been shown to be cytotoxic to human leukemia K562 cells with an IC_{50} in the low micromolar range.³⁵ The growth inhibitory effect of diazirine **2** was compared to etoposide in K562 cells after a 72 h continuous exposure. Diazirine **2** was 5.2-fold more cytotoxic than etoposide, with an IC_{50} of 0.42 μ M compared to that of etoposide of 2.2 μ M (Fig. 6A).

2.4. Topoisomerase II α inhibition and poisoning effects and topoisomerase I inhibition effects

The cytotoxicity of etoposide is due to its ability to convert topoisomerase II into a potent cellular poison.³⁶ The enzyme poisoning effect is achieved through stabilization of the cleavage complex, which inhibits the ability of the enzyme to religate the cleaved DNA strands,³⁷ leading to the formation of linear DNA. Etoposide-induced stabilization of the cleavage complex also results in inhibition of the catalytic strand passing activity of topoisomerase II. To determine whether diazirine **2** shares the same mechanism of action as etoposide by targeting topoisomerase II, the two compounds were compared for their ability to inhibit the catalytic activity of topoisomerase II, induce the formation of linear DNA, and produce protein–DNA covalent complexes.

The inhibition of topoisomerase II catalytic activity was determined by the ability of the drug to inhibit enzyme-mediated decatenation of kinetoplast plasmid DNA (kDNA) into mini circles of DNA.³⁸ In the assay, diazirine **2** showed twofold greater potency than etoposide, with an IC_{50} of 56 μ M compared to that of etoposide of 114 μ M (Fig. 6B). The topoisomerase II poisoning effect of diazirine **2** and etoposide was evaluated in a DNA cleavage assay.³⁹

As shown in Figure 6C, diazirine **2**, tested at 50 and 100 μ M, induced the formation of linear DNA to an extent similar to etoposide tested at 100 μ M.

To further confirm that diazirine **2** acts similarly to etoposide, we evaluated their effects on the level of covalent complex formations in intact K562 and K/VP.5 cells. The K/VP.5 cell line is a stable etoposide-resistant K562 cell line that contains one-fifth the topoisomerase II α protein content of the parental K562 cells.⁴⁰ Therefore, a topoisomerase II poison should produce a lower level of covalent complexes in K/VP.5 cells than in K562 cells. At tested concentrations of 50 μ M for etoposide and 80 μ M for diazirine **2**, protein–DNA covalent complexes were induced to a much lesser extent in K/VP.5 cells than in K562 cells, as shown in Figure 7A. These results are also consistent with our observation in the DNA cleavage assay (Fig. 6C) that diazirine **2** acts similarly to etoposide as a topoisomerase II poison.

The effects of diazirine **2** and etoposide on the inhibition of topoisomerase I-mediated relaxation of supercoiled DNA were also examined. Neither drug inhibited topoisomerase I at a tested concentration of 20 μ M, whereas camptothecin, a topoisomerase I inhibitor, at 50 μ M resulted in 40% inhibition (data not shown).

2.5. Effects of photolysis on drug-induced protein–DNA covalent complex formation

The stabilization of the cleavage complex by etoposide is a reversible process.⁴¹ Therefore, if diazirine **2** forms an irreversible covalent adduct with the cleavage complex, photolysis should increase the extent of cleavage complex formation by shifting the equilibrium process towards cleavage. Based on this hypothesis, we examined the effect of UV irradiation on etoposide- and diazirine 2-induced protein–DNA covalent complex formation in intact K562 cells (Fig. 7B). Incubation of cells with Diazirine **2** (2.5–20 μ M) resulted in a concentration dependent increase in covalent complex formation. UV irradiation significantly increased the levels of covalent complexes at all diazirine **2** concentrations ($p = 0.004$ – 0.031). In contrast, UV irradiation did not significantly affect the etoposide (25 μ M)-induced formation of covalent complexes at 25 μ M ($p = 0.793$).

3. Discussion

Diazirine **2** is a non-glycoside analog of etoposide and closely resembles the 4 β -benzoylamino derivatives of 4'-O-demethyl-4-

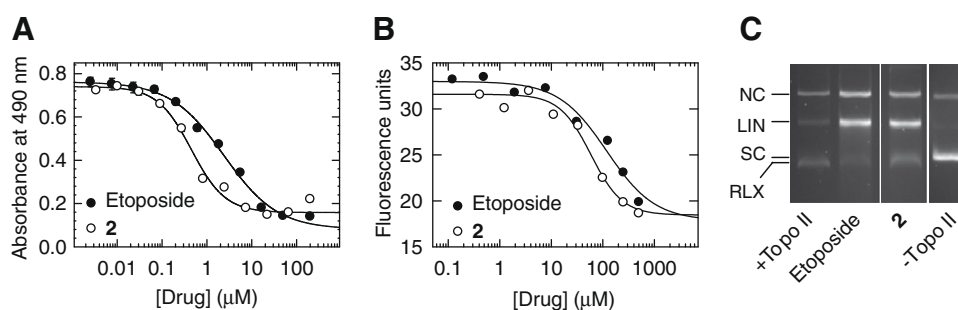


Figure 6. Comparison of the biological activity of diazirine **2** and etoposide in K562 cells and topoisomerase II assays. (A) The growth inhibitory effects of **2** (○) and etoposide (●) on K562 cells after a 72 h incubation as measured by an MTS assay. The curve lines are nonlinear least squares fits to a four-parameter logistic equation, and they yield IC_{50} 's of 0.42 ± 0.06 and 2.20 ± 0.41 μ M for **2** and etoposide, respectively. The values shown are triplicate determinations and where the error bars are not shown, they are smaller than the symbol. (B) The inhibitory effects of **2** (○) and etoposide (●) on the catalytic decatenation activity of topoisomerase II α . The fluorescence measures the amount of decatenated kDNA minicircles formed by the action of topoisomerase II α on kDNA. The curve solid lines are nonlinear least squares fit to a four-parameter logistic equation, and they yield IC_{50} 's of 56 ± 14 and 114 ± 53 μ M for **2** and etoposide, respectively. (C) The effect of **2** and etoposide on the topoisomerase II α -mediated cleavage of supercoiled pBR322 plasmid DNA. The grouping of three fluorescent images from different part of the same gel shows the ability of **2** and etoposide to induce the formation of linear DNA (LIN) at 100 μ M in the presence of topoisomerase II α (middle two lanes). The left lane of the gel shows that topoisomerase II α (+Topo II) relaxed supercoiled DNA (SC) to relaxed DNA (RLX) in the absence of drug, whereas the right lane shows the supercoiled pBR322 DNA in the absence of the enzyme and drug (-Topo II). A small amount of nicked circular DNA (NC) is normally present in the pBR322 DNA.

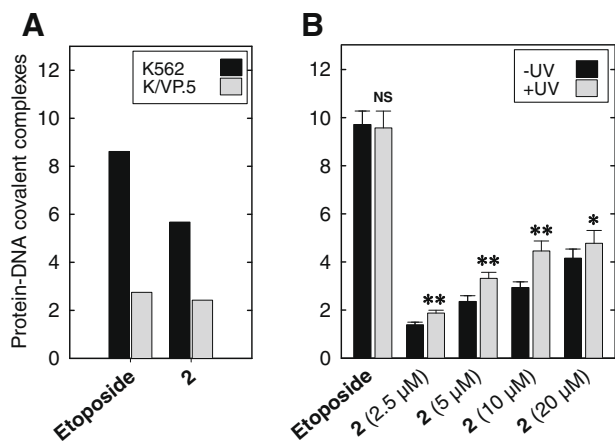


Figure 7. Comparison of the effects of **2** and etoposide on the formation of topoisomerase II–DNA covalent complexes in intact cells. Results are shown as protein–DNA covalent complexes formation induced by etoposide or **2**. (A) Comparison of drug-induced protein–DNA covalent complexes in K562 cells and the etoposide-resistant K/VP.5 cells containing decreased levels of topoisomerase II α . Diazirine **2** at 80 μ M and etoposide at 50 μ M induced the formation of covalent complexes to a lesser extent in K/VP.5 cells than in K562 cells. (B) Effect of UV irradiation on **2**- and etoposide-induced formation of covalent complexes in K562 cells. Diazirine **2** (2.5–20 μ M), etoposide (25 μ M), or DMSO were added to suspensions of K562 cells then immediately irradiated (or not), as indicated, at 365 nm for 5 min. Cells were then incubated for 60 min at 37 $^{\circ}$ C in the dark followed by processing for protein–DNA covalent complex formation as described in Section 4. Bars represent the mean \pm SEM from nine different experiments performed on different days. Paired *t*-tests were performed for each drug concentration in the presence compared to the absence of UV light. The * and ** indicate *p* < 0.05 and 0.01, respectively. NS indicates not significant. The results show that the increase of the levels of drug-induced covalent complexes by UV irradiation at all four concentrations of diazirine **2** is statistically significant. However, UV irradiation did not have any significant effect on the etoposide-induced formation of covalent complexes.

desoxytopodophyllotoxin reported in the literature.^{42,43} Although diazirine **2** is structurally different than etoposide, we anticipate that diazirine **2** will bind to topoisomerase II in a manner similar to etoposide. In support of this idea, the 4 β -benzoylamino derivatives have been shown to be cytotoxic and share similar mechanism of action as etoposide by acting as topoisomerase II poisons.⁴³ Another non-glycoside analog of etoposide, Top-53 (Fig. 1A), which is also structurally different than etoposide at the 4 β -position, has been shown to compete with etoposide in binding to topoisomerase II in a competitive binding assay.⁴⁴ In addition, the binding of Top-53 to topoisomerase II has been shown in an NMR spectroscopy study.⁴⁴ These findings support further proteomic studies to characterize the binding of diazirine **2** to topoisomerase II.

The 3-trifluoromethyl-3-aryldiazirine group is the photophore of choice for our photoaffinity etoposide probe for several reasons. The diazirines are known to be readily photoactivatable to produce highly reactive carbene species that should enhance the probability of labeling drug binding sites and reduce non-specific labeling caused by migration of the labeling probe from the binding pocket.^{22–24} Another advantage of diazirines is that their photolysis always gives rise to photoadducts with carbon-based covalent bonds that should be stable in the subsequent protein sequencing steps and MALDI-MS experiments. Lastly, the photoactivation of diazirine can be readily achieved with a short photoirradiation time and at near UV wavelengths (e.g., 365 nm) with less potential to cause UV-induced protein or cellular damage. Although the diazirine photophore can undergo photorearrangement to afford the longer lived diazo isomer as a side product, the diazo isomer can be rapidly converted into a reactive carbene intermediate by a subsequent photolysis at 302 nm.³⁴

Diazirine **2**, which was conveniently synthesized in three steps from commercially available podophyllotoxin **3** and benzoic acid **6**, exhibited the desirable photoaffinity labeling properties described above. This conclusion is made on the basis of our findings obtained in the photochemical kinetic and LC–MS/MS studies. Diazirine **2** underwent facile photolysis in solution, with reaction completed in 600 s upon continuous irradiation at 365 nm. The sequential application of irradiation at wavelengths of 365 and then 302 nm, which has also been applied by Hosoya et al. on their diazirine probe,³⁴ significantly shortened the photoirradiation time of **2** for reaching complete photolysis to only 120 s. The increased photolysis efficiency of **2** by nearly fivefold under this condition should improve the labeling yield of diazirine **2** on topoisomerase II, which in turn should enhance the detection of labeled peptide fragments. The carbene intermediate generated photochemically from diazirine **2** or diazo **8** reacted with methanol and molecular oxygen or water to form carbon–oxygen photoadducts that were readily detected using LC–MS/MS. The high abundances of the molecular ions of these photoadducts in ESI–MS mode suggest that the loss of probe **2** via carbon–heteroatom bond cleavage from the labeled peptide under MALDI–MS conditions should be minimal. The carbene intermediate was also shown to react with ethyl acetate and acetonitrile to afford photoadducts with highly stable carbon–carbon bonds. The ability of the carbene to insert into aliphatic C–H bonds is indicative of the formation of an extremely reactive species, and suggests that diazirine **2** should be useful as a photoaffinity probe.

Several lines of evidence obtained for non-glycoside etoposide analogs^{42–44} support our hypothesis that diazirine **2** interacts with topoisomerase II in a manner similar to etoposide. The biological studies we conducted for **2** and etoposide further validate our hypothesis. Diazirine **2** exhibited five- and twofold greater potency than etoposide in the K562 cell growth inhibition assay and the topoisomerase II catalytic inhibition assay, respectively. The slightly greater potency of diazirine **2** observed in the cell inhibition assay may be the result of increased cellular drug uptake because of the higher lipophilicity of the drug compared to etoposide. Overall, diazirine **2** and etoposide exhibited comparable levels of potency in these two assays. In addition, diazirine **2** was able to induce linear DNA formation at levels comparable to that for etoposide. Diazirine **2** also shared a similar profile as etoposide in the induction of protein–DNA covalent complexes in K562 and K/VP.5 cells. Taken together, our results are consistent with diazirine **2** exhibiting similar biological activities as etoposide. Our results and the fact that diazirine **2** is structurally related to etoposide strongly support the hypothesis that both drugs interact with topoisomerase II in a similar manner. The fact that diazirine **2** significantly increased covalent complex formation after the cells were exposed to UV irradiation strongly suggests that diazirine **2** formed a covalent adduct with topoisomerase II.

In conclusion, our results demonstrate that diazirine **2** should prove useful for identifying the etoposide binding sites on topoisomerase II. The photoaffinity labeling of purified human topoisomerase II α with diazirine **2** and the subsequent identification of labeled amino acid residues using a proteomics mass spectrometry approach are underway.

4. Experimental section

4.1. Chemical synthesis of *N*-[(10*S*,11*S*,15*R*,16*R*)-16-(4-hydroxy-3,5-dimethoxyphenyl)-14-oxo-4,6,13-trioxatetracyclo[7.7.0.0.3⁷.0^{11,15}]hexadeca-1,3(7),8-trien-10-yl]-4-[3-(trifluoromethyl)-3*H*-diazirin-3-yl]benzamide (**2**)

Reactants **3** and **6** (Fig. 1A and B) were purchased from Avachem Scientific LLC (San Antonio, TX), and Bachem Americas Inc.

(Torrance, CA), respectively. All other reagents were from Sigma–Aldrich (St. Louis, MO). ^1H and ^{13}C NMR spectra were recorded on a Bruker AM-300 FT instrument. High resolution mass spectrum (HRMS) was recorded on an Agilent 6210 Time-of-flight LC–MS instrument. Preparative thin layer chromatography was carried out on Fisher silica gel plates with fluorescent indicator (layer thickness 250 μm , particle size 5–17 μm , pore size 60 \AA , and plate dimension 20 \times 20 cm). All reactions involving the diazirine derivatives were carried out under reduced light because of their photosensitivity. Amine **5** was prepared from podophyllotoxin **3** via azide **4** according to a previously reported procedure.²⁵ The amine was then reacted with acyl chloride **7**,⁴⁵ which was in turn prepared from **6**, to afford diazirine **2** as described in the following procedure. Carboxylic acid **6** (23 mg, 0.1 mmol) was dissolved in thionyl chloride (0.2 ml), and the resulting solution was stirred at room temperature for 20 h. The distillation to remove the excess thionyl chloride was carefully performed at a reduced pressure of not lower than 40 mbar for about 20 min at 25 $^\circ\text{C}$ to maximize the removal of thionyl chloride without leading to excessive loss of the volatile acyl chloride **7**.⁴⁵ The resulting liquid residue was dissolved in ethyl acetate (0.1 ml) and added dropwise to a stirred solution of amine **5** (40 mg, 0.1 mmol) and pyridine (23 μl , 0.28 mmol) in ethyl acetate (0.2 ml). After stirring at room temperature for 1 h, the resulting suspension was filtered, concentrated to about 0.1 ml, and chromatographed on a preparative TLC plate with 60% ethyl acetate/hexanes. The desired band on the plate was detected in a dark room briefly under an indirect 254 nm UV light from a hand-held lamp. The band was scraped out, eluted with ethyl acetate, and concentrated to afford **2** as a beige solid (25 mg, 41% yield). ^1H NMR (300 MHz, CDCl_3) δ 2.90 (1H, dd, $J = 4.9, 14.3$), 3.03 (1H, m), 3.77 (6H, s), 3.85 (1H, dd, $J = 9.5, 10.4$), 4.47 (1H, dd, $J = 7.6, 9.1$), 4.59 (1H, d, $J = 4.8$), 5.42 (2H, dd, $J = 5.2, 5.3$), 5.98 (2H, AB, $\Delta\delta = 6.9, J = 1.1$), 6.27 (1H, d, 7.0), 6.31 (2H, s), 6.56 (1H, s), 6.79 (1H, s), 7.27 (2H, d, $J = 8.0$), 7.81 (2H, d, $J = 8.5$); ^{13}C NMR (75.5 MHz, CDCl_3) δ 28.5 (CN_2 , q, $J = 41$), 37.4 (CH), 42.0 (CH), 43.6 (CH), 48.9 (CH), 56.5 ($2 \times \text{CH}_3$), 69.1 (CH_2), 101.7 (CH_2), 107.9 (CH), 108.9 (CH), 110.3 ($2 \times \text{CH}$), 122.6 (CF_3 , q, $J = 273$) 126.8 ($2 \times \text{CH}$), 127.6 ($2 \times \text{CH}$), 128.5 (C), 130.1 (C), 132.9 (C), 133.2 (C), 134.1 (C), 134.2 (C), 146.5 ($2 \times \text{C}$), 147.8 (C), 148.6 (C), 166.2 (C), 174.2 (C); ESI tandem mass spectrum m/z (relative intensity) 612 ($[\text{M}+\text{H}]^+$, 77), 584 (100), 383 (18); HRMS calcd for $[\text{C}_{30}\text{H}_{24}\text{F}_3\text{N}_3\text{O}_8+\text{H}]^+$ 612.1593, found 612.1590.

4.2. Photochemical kinetics in organic solvents

The photochemical reactions of diazirine **2** were carried out at 80 μM in selected solvents, as indicated, in 1-cm stoppered silica cells placed on the surface of the transilluminator in an Alpha Innotech Fluorchem 8900 imaging system (6.2 and 4.5 mW/cm^2 at 302 and 365 nm, respectively, at the surface). The solutions were exposed to the UV light at selected wavelengths, as indicated, for fixed times and the UV–vis spectra were recorded on a Cary 1 spectrophotometer (Varian, Mulgrave, Australia).

4.3. LC–MS/MS analysis of photolysis products produced in organic solvents

Photolyzed diazirine **2** in methanol or acetonitrile, as indicated, was directly diluted with water to give an 80% organic solvent/water solution with a concentration of 64 μM (on a reactant basis). Photolyzed **2** in ethyl acetate was concentrated to dryness and redissolved in 80% methanol/water to afford the same concentration. The solutions were then analyzed with a Varian 500-MS LC–MS/MS ion trap mass spectrometer equipped with 212-LC chromatography equipment using the following analytical conditions. The isocratic eluent was 60% (v/v) methanol/water containing 0.1% (v/

v) formic acid with a flow rate of 200 $\mu\text{l}/\text{min}$. The sample (10 μl) was chromatographed on a Varian Pursuit C-18 column (3 μm pore size, 100 \times 2 mm). The ionization mode was ESI positive with N_2 at 50 psi as the nebulizer gas. The drying gas was set at 50 psi and 350 $^\circ\text{C}$. The voltages of the needle and shield were 5000 and 80 V, respectively. Positive ions were scanned in the range of 200–760 Da using a scan rate of 15 kDa/s and a mass increment of 150–2000 Da. The relevant precursor ions were selected for low energy collision-induced dissociation MS/MS analyses using helium as the collision gas with a flow rate of 0.8 ml/min and collision voltage in the range of 0.5–2.5 V.

4.4. Cell culture and growth inhibition assay

K562 cells were obtained from American Type Culture Collection (Rockville, MD). K/VP.5 cells are a 26-fold etoposide-resistant K562-derived sub-line with decreased levels of topoisomerase II α mRNA and protein.⁴⁰ These cells were maintained as suspension cultures in alpha minimum essential medium (αMEM) (Gibco BRL, Burlington, Canada) containing 2 mM L-glutamine and supplemented with 10% fetal calf serum (Invitrogen, Burlington, ON, Canada), 20 mM NaHCO_3 , 20 mM HEPES (Sigma), 100 units/ml penicillin G, and 100 $\mu\text{g}/\text{ml}$ streptomycin at pH 7.4 in an atmosphere of 5% CO_2 and 95% air at 37 $^\circ\text{C}$. For the measurement of growth inhibition, cells in exponential growth were harvested and seeded at 6000 cells/well in 96-well plates (100 $\mu\text{l}/\text{well}$). Diazirine **2** and etoposide were dissolved in DMSO and added to the wells such that the final concentration of DMSO was 0.5% (v/v). After 72 h incubation, 7 μl of 3-(4,5-dimethylthiazol-2-yl)-5-(3-carboxymethoxyphenyl)-2-(4-sulfophenyl)-2H-tetrazolium (MTS) Cell Titer 96[®] Aqueous One Solution (Promega, MD, WI) was added to each well and incubated for a further 3 h. The absorbance was measured in a Molecular Devices (Menlo Park, CA) plate reader. The spectrophotometric 96-well plate cell growth inhibition assay measures the ability of the cells to enzymatically reduce MTS. Three replicates were measured at each drug concentration, and the IC_{50} values and their SEs for growth inhibition were obtained by fitting the absorbance–drug concentration data to a four-parameter logistic equation as we previously described.⁴⁶

4.5. Topoisomerase II α decatenation and topoisomerase I relaxation inhibition assays

The catalytic inhibition of purified human topoisomerase II α by diazirine **2** and etoposide was measured by the ATP-dependent decatenation of kDNA (Topogen, Columbus, OH) into minicircles of DNA as we previously described.³⁸ The reaction mixture contained 0.5 mM ATP, 50 mM Tris–HCl (pH 8.0), 120 mM KCl, 10 mM MgCl_2 , 30 $\mu\text{g}/\text{ml}$ bovine serum albumin, 40 ng kDNA, diazirine **2**, etoposide, or DMSO (0.5 μl) and 18 ng human topoisomerase II α protein (an amount that gave 80% decatenation). The enzyme was expressed using a high copy yeast expression vector, extracted, and purified as we previously described.³⁸ The enzymatic reaction was carried out at 37 $^\circ\text{C}$ and was terminated by the addition of 12 μl of 250 mM EDTA. Samples were centrifuged at 8000g at 25 $^\circ\text{C}$ for 15 min and 20 μl of the supernatant was added to 180 μl of 600-fold diluted PicoGreen dye (Molecular Probes, Eugene, OR) in a 96-well black plate with a clear bottom. The fluorescence, which is proportional to the amount of decatenated kDNA, was measured in a Fluostar Galaxy (BMG, Durham, NC) fluorescent plate reader using an excitation wavelength of 485 nm and an emission wavelength of 520 nm. The IC_{50} values and their SEs for decatenation inhibition were obtained by fitting the fluorescence unit–drug concentration data to a four-parameter logistic equation as we previously described.⁴⁶ The catalytic inhibition of topoisomerase I in K562 nuclear extract by diazirine **2** and

etoposide was measured using a procedure we described previously.⁴⁷

4.6. Topoisomerase II α DNA cleavage assay

Topoisomerase II-cleaved DNA covalent complexes induced by topoisomerase II poisons such as etoposide may be trapped by rapidly denaturing the complexed enzyme with sodium dodecyl sulfate (SDS), thus releasing the cleaved DNA as linear DNA.^{41,48} The formation of linear DNA was detected by separating the SDS-treated reaction products using ethidium bromide gel electrophoresis as described previously.⁴⁹ The band corresponding to linear DNA was identified by comparison with that from linear pBR322 DNA produced by action of the restriction enzyme HindIII acting on a single site on pBR322 DNA. The 20 μ l cleavage assay reaction mixture³⁹ contained 150 ng topoisomerase II α protein, 80 ng pBR322 plasmid DNA (MBI Fermentas, Burlington, ON, Canada), 0.5 mM ATP in assay buffer (10 mM Tris–HCl, 50 mM KCl, 50 mM NaCl, 0.1 mM EDTA, 5 mM MgCl₂, 2.5% glycerol, at pH 8.0), and typically 50–100 μ M of the drug (0.5 μ l in DMSO), as indicated. The order of addition was assay buffer, DNA, topoisomerase II α , and then drug. The mixture was assembled on ice before the addition of drug solution. The reaction mixture was incubated at 37 °C for 10 min, and then quenched with 0.05% (v/v) SDS/22 mM EDTA. The mixture was subsequently treated with 0.25 mg/ml proteinase K (Sigma) at 55 °C for 30 min to digest the topoisomerase II α protein, and was separated by electrophoresis (2 h at 8 V/cm) on an agarose gel prepared from 1.2% w/v agarose and 0.5 μ g/ml ethidium bromide in TAE buffer pH 8.0 (40 mM Tris base, 0.114% (v/v) glacial acetic acid, 2 mM EDTA). The DNA in the gel was imaged by its fluorescence on an Alpha Annotech Fluorchem 8900 imaging system equipped with a 365 nm illuminator and a CCD camera.

4.7. Protein–DNA covalent complexes formation assay

Topoisomerase II–DNA covalent complex formation in intact K562 or K/VP.5 cells, with or without UV irradiation, as indicated, was measured as we previously described.²¹ Briefly, mid-log growth cells were radiolabeled for 24 h with 0.5 μ Ci/ml [methyl-³H]thymidine (0.5 Ci/mmol) and 0.1 μ Ci/ml [¹⁴C]leucine (318 mCi/mmol) in Dulbecco's modified Eagle's medium (DMEM) containing 7.5% (v/v) iron-supplemented calf serum. The cells were pelleted, resuspended in fresh DMEM/7.5% (v/v) calf serum, and incubated for 1 h at 37 °C. They were pelleted again and incubated in buffer (pH 7.4) containing 25 mM HEPES, 115 mM NaCl, 5 mM KCl, 1 mM MgCl₂, 5 mM NaH₂PO₄ and 10 mM glucose in 24-well plates at 37 °C at a final cell density of 1.5×10^6 cells/ml for experimentation. The height of the cell suspension in 24-well plates was 4.5 mm for all experiments. The cells were then exposed to diazirine **2**, etoposide, or DMSO, immediately irradiated (or not) at 365 nm for 5 min using a UVL-21 hand lamp (0.32 mW/cm² at 365 nm at 152 mm distance) from a distance of 16 mm to the liquid surface of the cell suspension. Cells were then incubated at 37 °C for an additional 60 min in the dark. Cellular processes were quenched by adding the cells to ice-cold PBS at 10 \times volume. The cells were then pelleted, lysed, cellular DNA sheared, and protein–DNA complexes precipitated with SDS and KCl as described by Zwelling et al.⁵⁰ Protein–DNA complexes were quantified by scintillation counting and [³H]DNA was normalized to cell number using the co-precipitated ¹⁴C-labeled protein as an internal control. Results are presented as protein–DNA complexes in the presence of drug minus those found in DMSO controls.

Acknowledgments

This work was supported by institutional grants from the University of Manitoba, Canadian Institutes of Health Research, Na-

tional Institutes of Health grant CA090787 to J.C.Y. and a Canada Research Chair for Drug Development for B.B.H. We also acknowledge the assistance of Drs. Tom Ward and Rui Zhang for providing LC–MS/MS technical support and acquiring NMR spectra, respectively.

Supplementary data

Supplementary data (spectroscopic data of diazirine **2** is provided) associated with this article can be found, in the online version, at doi:10.1016/j.bmc.2009.11.048.

References and notes

- Belani, C. P.; Doyle, L. A.; Aisner, J. *Cancer Chemother. Pharmacol.* **1994**, *34*, 5118.
- Hande, K. R. *Eur. J. Cancer* **1998**, *34*, 1514.
- Meresse, P.; Dechaux, E.; Monneret, C.; Bertounesque, E. *Curr. Med. Chem.* **2004**, *11*, 2443.
- Fortune, J. M.; Osheroff, N. *Prog. Nucleic Acid Res. Mol. Biol.* **2000**, *64*, 221.
- Nitiss, J. L. *Biochim. Biophys. Acta* **1998**, *1400*, 63.
- Wang, J. C. *Nat. Rev. Mol. Cell Biol.* **2002**, *3*, 430.
- Felix, C. A.; Kolaris, C. P.; Osheroff, N. *DNA Repair (Amst)* **2006**, *5*, 1093.
- Sordet, O.; Khan, Q. A.; Kohn, K. W.; Pommier, Y. *Curr. Med. Chem. Anticancer Agents* **2003**, *3*, 271.
- Wilstermann, A. M.; Osheroff, N. *Curr. Top. Med. Chem.* **2003**, *3*, 321.
- Berger, J. M. *Biochim. Biophys. Acta* **1998**, *1400*, 3.
- Berger, J. M.; Gamblin, S. J.; Harrison, S. C.; Wang, J. C. *Nature* **1996**, *379*, 225.
- Berger, J. M.; Wang, J. C. *Curr. Opin. Struct. Biol.* **1996**, *6*, 84.
- Dong, K. C.; Berger, J. M. *Nature* **2007**, *450*, 1201.
- Fass, D.; Bogden, C. E.; Berger, J. M. *Nat. Struct. Biol.* **1999**, *6*, 322.
- Schoeffler, A. J.; Berger, J. M. *Q. Rev. Biophys.* **2008**, *41*, 41.
- Holthuis, J. J. M. *Pharm. Weekbl Sci.* **1988**, *10*, 101.
- Liu, Y.-Q.; Yang, L.; Tian, X. *Curr. Bioactive Compd.* **2007**, *3*, 37.
- Gordaliza, M.; Garcia, P. A.; del Corral, J. M.; Castro, M. A.; Gomez-Zurita, M. A. *Toxicol* **2004**, *44*, 441.
- Kingma, P. S.; Burden, D. A.; Osheroff, N. *Biochemistry* **1999**, *38*, 3457.
- Leroy, D.; Kajava, A. V.; Frei, C.; Gasser, S. M. *Biochemistry* **2001**, *40*, 1624.
- Hasinoff, B. B.; Chee, G. L.; Day, B. W.; Avor, K. S.; Barnabé, N.; Thampatty, P.; Yalowich, J. C. *Bioorg. Med. Chem.* **2001**, *9*, 1765.
- Hatanaka, Y.; Nakayama, H.; Kanaoka, Y. *Rev. Heteroat. Chem.* **1996**, *14*, 213.
- Hatanaka, Y.; Sadakane, Y. *Curr. Top. Med. Chem.* **2002**, *2*, 271.
- Hashimoto, M.; Hatanaka, Y. *Eur. J. Org. Chem.* **2008**, 2513.
- Hansen, H. F.; Jensen, R. B.; Willumsen, A. M.; Nørskov-Lauritsen, N.; Ebbesen, P.; Nielsen, P. E.; Buchardt, O. *Acta Chem. Scand.* **1993**, *47*, 1190.
- Ambrose, Y.; Pillon, F.; Mioskowski, C.; Valleix, A.; Rousseau, B. *Eur. J. Org. Chem.* **2001**, 3961.
- Burgermeister, W.; Nassal, M.; Wieland, T.; Helmreich, E. J. M. *Biochim. Biophys. Acta* **1983**, *729*, 219.
- Hatanaka, Y.; Hashimoto, M.; Nakayama, H.; Kanaoka, Y. *Chem. Pharm. Bull.* **1994**, *42*, 826.
- Weber, T.; Brunner, J. J. *Am. Chem. Soc.* **1995**, *117*, 3084.
- Nassal, M. J. *Am. Chem. Soc.* **1984**, *106*, 7540.
- Brunner, J.; Senn, H.; Richards, F. M. *J. Biol. Chem.* **1980**, *255*, 3313.
- Li, Q.; Yan, G.; Ge, T. *Rapid Commun. Mass Spectrom.* **2007**, *21*, 2843.
- Mathur, N. C.; Snow, M. S.; Young, K. M.; Pincock, J. A. *Tetrahedron Lett.* **1985**, *41*, 1509.
- Hosoya, T.; Hiramatsu, T.; Ikemoto, T.; Nakanishi, M.; Aoyama, H.; Hosoya, A.; Iwata, T.; Maruyama, K.; Endo, M.; Suzuki, M. *Org. Biomol. Chem.* **2004**, *2*, 637.
- Chao, N. J.; Aihara, M.; Blume, K. G.; Sikic, B. I. *Exp. Hematol.* **1990**, *18*, 1193.
- Froelich-Ammon, S. J.; Osheroff, N. *J. Biol. Chem.* **1995**, *270*, 21429.
- Kingma, P. S.; Osheroff, N. *J. Biol. Chem.* **1997**, *272*, 1148.
- Hasinoff, B. B.; Wu, X.; Krokhin, O. V.; Ens, W.; Standing, K. G.; Nitiss, J. L.; Sivaram, T.; Giorgianni, A.; Yang, S.; Jiang, Y.; Yalowich, J. C. *Mol. Pharmacol.* **2005**, *67*, 937.
- Liang, H.; Wu, X.; Guziec, L. J.; Guziec, F. S., Jr.; Larson, K. K.; Lang, J.; Yalowich, J. C.; Hasinoff, B. B. *J. Chem. Info. Model.* **2006**, *46*, 1827.
- Ritke, M. K.; Roberts, D.; Allan, W. P.; Raymond, J.; Bergoltz, V. V.; Yalowich, J. C. *Br. J. Cancer* **1994**, *69*, 687.
- Osheroff, N. *Biochemistry* **1989**, *28*, 6157.
- Xu, H.; Lv, M.; Tian, X. *Curr. Med. Chem.* **2009**, *16*, 327.
- Zhou, X. M.; Wang, Z. Q.; Chen, H. X.; Cheng, Y. C.; Lee, K. H. *Pharm. Res.* **1993**, *10*, 214.
- Wilstermann, A. M.; Bender, R. P.; Godfrey, M.; Choi, S.; Anklin, C.; Berkowitz, D. B.; Osheroff, N.; Graves, D. E. *Biochemistry* **2007**, *46*, 8217.
- Bender, T.; Huss, M.; Wiecezorek, H.; Grond, S.; Von Zezschwitz, P. *Eur. J. Org. Chem.* **2007**, 3870.

46. Hasinoff, B. B.; Creighton, A. M.; Kozłowska, H.; Thampatty, P.; Allan, W. P.; Yalowich, J. C. *Mol. Pharmacol.* **1997**, *52*, 839.
47. Hasinoff, B. B.; Wu, X.; Yalowich, J. C.; Goodfellow, V.; Laufer, R. S.; Adedayo, O.; Dmitrienko, G. I. *Anti-Cancer Drugs* **2006**, *17*, 825.
48. Osheroﬀ, N.; Zechiedrich, E. L. *Biochemistry* **1987**, *26*, 4303.
49. Burden, D. A.; Froelich-Ammon, S. J.; Osheroﬀ, N. *Methods Mol. Biol.* **2001**, *95*, 283.
50. Zwelling, L. A.; Hinds, M.; Chan, D.; Mayes, J.; Sie, K. L.; Parker, E.; Silberman, L.; Radcliffe, A.; Beran, M.; Blick, M. *J. Biol. Chem.* **1989**, *264*, 16411.